

Stress states and moment rates of a two-asperity fault in the presence of viscoelastic relaxation

M. Dragoni and E. Lorenzano

Dipartimento di Fisica e Astronomia, Alma Mater Studiorum Università di Bologna, Viale Carlo Bertini Pichat 8, 40127 Bologna, Italy

Abstract

A fault containing two asperities with different strengths is considered. The fault is embedded in a shear zone subject to a constant strain rate by the motions of adjacent tectonic plates. The fault is modelled as a discrete dynamical system where the average values of stress, friction and slip on each asperity are considered. The state of the fault is described by three variables: the slip deficits of the asperities and the viscoelastic deformation. The system has four dynamic modes, for which analytical solutions are calculated. The relationship between the state of the fault before a seismic event and the sequence of slipping modes in the event is enlightened. Since the moment rate depends on the number and sequence of slipping modes, the knowledge of the source function of an earthquake constrains the orbit of the system in the phase space. If the source functions of a larger number of consecutive earthquakes were known, the orbit could be constrained more and more and its evolution could be predicted with a smaller

17 uncertainty. The model is applied to the 1964 Alaska earthquake,
18 which was the effect of the failure of two asperities and for which a
19 remarkable postseismic relaxation has been observed in the subsequent
20 decades. The evolution of the system after the 1964 event depends on
21 the state from which the event was originated, that is constrained by
22 the observed moment rate. The possible durations of the interseismic
23 interval and the possible moment rates of the next earthquake are
24 calculated as functions of the initial state.

25 **1 Introduction**

26 Many aspects of fault dynamics can be reproduced by asperity models (Lay et
27 al., 1982; Scholz, 1990), assuming that one or more regions of the fault have
28 a much higher friction than the adjacent regions. Several large and medium-
29 size earthquakes that occurred in the last decades were the result of the failure
30 of two distinct asperities, such as the 1964 Alaska earthquake (Christensen
31 and Beck, 1994), the 1995 Kobe earthquake (Kikuchi and Kanamori, 1996),
32 the 2004 Parkfield earthquake (Johanson et al., 2006) and the 2010 Maule,
33 Chile, earthquake (Delouis et al., 2010).

34 In the framework of an asperity model, the evolution of asperities in
35 terms of stress accumulation, seismic slip and mutual stress transfer plays
36 a key role. Therefore the dynamical behaviour of a fault can be fruitfully
37 investigated by means of discrete models describing the state of asperities
38 (e.g. Ruff, 1992; Rice, 1993; Turcotte, 1997). An advantage associated with
39 a finite number of degrees of freedom is that we can predict the evolution of
40 the system at long term by calculating its orbit in the phase space.

41 A discrete fault model with two asperities was originally proposed by
42 Nussbaum and Ruina (1987) and further investigated by Huang and Turcotte
43 (1990, 1992), McCloskey and Bean (1992) and others. Dragoni and Santini
44 (2012, 2014) solved analytically the equations of motion in the case of a
45 two-asperity fault with different strengths in an elastic medium.

46 In the long-term evolution of a fault, the rheological properties of the
47 Earth's lithosphere play an important role. Lithospheric rocks are not per-
48 fectly elastic, but have a certain degree of anelasticity (Carter, 1976; Kirby
49 and Kronenberg, 1987; Ranalli, 1995; Nishimura and Thatcher, 2003; Bürg-
50 mann and Dresen, 2008). As a consequence, the static stress fields produced
51 by fault dislocations undergo a certain amount of relaxation during the inter-
52 seismic intervals, which alters the stress distribution on faults and modifies
53 the occurrence times of seismic events (Kusznir, 1991; Kenner and Segall,
54 2000; Smith and Sandwell, 2006; Piombo et al., 2007; Ding and Lin, 2014).

55 A preliminary study of the effects of viscoelastic relaxation on a fault
56 containing two asperities was made by Amendola and Dragoni (2013), in
57 the case of asperities with the same frictional strength. It was shown that
58 the stresses on the asperities increase non-linearly during the interseismic
59 intervals, although the tectonic loading takes place at constant rate. As
60 a consequence, earthquakes are anticipated or delayed with respect to the
61 case of an elastic medium. In addition, the stress rate is different for the
62 two asperities, so that the stress distribution changes during loading and
63 the asperity subject to the greater stress at a given instant of time is not
64 necessarily the first one to fail in the next earthquake.

65 The present paper generalizes Amendola and Dragoni (2013) in that it
66 considers two asperities with different strengths and a larger set of possible
67 states for the fault in the interseismic intervals. We investigate which subsets
68 of states drive the system to the failure of one asperity or both. Whether the
69 failure starts at one asperity or the other has consequences on the position of
70 the earthquake focus as well as on its source function and seismic moment.

71 The model is applied to the 1964 Alaska earthquake, for which a suffi-
72 ciently long time interval has elapsed to allow observation of a remarkable
73 postseismic relaxation (Zweck et al., 2002). The moment rate of the earth-
74 quake was modelled by Dragoni and Santini (2012), showing that it can be
75 approximately represented as a 2-mode event with the consecutive failure of
76 the two asperities. We study the subsequent evolution of the system in the
77 presence of viscoelastic relaxation and calculate the duration of the interseis-
78 mic interval and the possible source functions of the next earthquake.

79 **2 The model**

80 We consider a plane fault with two asperities of equal areas, that we name
81 asperity 1 and 2 respectively (Fig. 1). Following Amendola and Dragoni
82 (2013), all quantities are expressed in nondimensional form. We assume that
83 the fault is embedded in a homogeneous and isotropic shear zone, subject to
84 a uniform strain rate by the motion of two tectonic plates at relative velocity
85 V . The rheological properties of the lithosphere are taken into account by
86 assuming that coseismic stresses are relaxed with a characteristic Maxwell
87 time Θ .

88 We do not determine stress, friction and slip at every point of the fault
89 but, instead, the average values of these quantities on each asperity. We
90 define the slip deficit of an asperity at a certain instant T of time as the
91 slip that the asperity should undergo in order to recover the relative plate
92 displacement occurred up to time T .

93 The state of the fault is described by three variables X , Y and Z , where
94 X and Y are the slip deficits of asperities 1 and 2 respectively, while Z is
95 viscoelastic deformation. Accordingly, the asperities are subject to tangential
96 forces

$$F_1 = -X + \alpha Z, \quad F_2 = -Y - \alpha Z \quad (1)$$

97 where α is a coupling constant and the terms $\pm\alpha Z$ are the contribution of
98 stress transfer between the asperities in the presence of viscoelastic deforma-
99 tion. The couple (F_1, F_2) yields the stress state of the fault.

100 The forces F_1 e F_2 are defined as the forces that act on the asperities in
101 the slip direction: therefore they are valid for any source mechanism (strike-
102 slip, dip-slip or other). In equation (1), the terms $-X$ and $-Y$ represent the
103 tectonic loading of asperity 1 and 2 respectively and have the same sign for
104 both asperities. In the expression for F_1 , the term αZ is the force applied to
105 asperity 1 by the past motions of asperities, in the presence of viscoelastic
106 relaxation. Analogously, in the expression for F_2 , the term $-\alpha Z$ is the force
107 applied to asperity 2 by the past motions of asperities.

108 Fault slip is governed by friction, that is best described by the rate-and-
109 state friction laws (Ruina, 1983; Dieterich, 1994). According to the premise,
110 we use a simpler law assuming that the asperities are characterized by con-

111 stant static frictions and consider the average values of dynamic frictions
 112 during fault slip. We assume that the static friction of asperity 2 is a frac-
 113 tion β of that of asperity 1 and that dynamic frictions are a fraction ϵ of
 114 static frictions.

115 If we call f_{s1} and f_{d1} the static and the dynamic frictions of asperity 1,
 116 respectively, and f_{s2} and f_{d2} the static and the dynamic frictions of asperity
 117 2, we define

$$\epsilon = \frac{f_{d1}}{f_{s1}} = \frac{f_{d2}}{f_{s2}} \quad (2)$$

118 and

$$\beta = \frac{f_{s2}}{f_{s1}} = \frac{f_{d2}}{f_{d1}} \quad (3)$$

119 Hence the system is described by the five parameters α , β , ϵ , Θ and V , with
 120 $\alpha > 0$, $0 < \beta < 1$, $0 < \epsilon < 1$, $\Theta > 0$, $V > 0$. From these parameters we can
 121 define a slip

$$U = 2 \frac{1 - \epsilon}{1 + \alpha} \quad (4)$$

122 and the frequencies

$$\omega = \sqrt{1 + \alpha}, \quad \Omega = \sqrt{1 + 2\alpha} \quad (5)$$

123 that will appear in the solutions. The system is subject to the additional
 124 constraint

$$X \geq 0, \quad Y \geq 0 \quad (6)$$

125 that excludes overshooting during fault slip. Forces are expressed in terms
 126 of the static friction of asperity 1, so that the conditions for the failure of
 127 asperities 1 and 2 are respectively

$$F_1 = -1, \quad F_2 = -\beta \quad (7)$$

128 or, from (1),

$$129 \quad X - \alpha Z - 1 = 0 \quad (8)$$

$$Y + \alpha Z - \beta = 0 \quad (9)$$

130 These are the equations of two planes in the space XYZ , that we call Π_1
131 and Π_2 respectively.

132 The dynamics of the system has four different modes: a sticking mode,
133 corresponding to stationary asperities (mode 00), and three slipping modes,
134 corresponding to the failure of asperity 1 (mode 10), the failure of asperity 2
135 (mode 01), and the simultaneous failure of both asperities (mode 11). Each
136 mode is described by a different system of differential equations.

137 In mode 00, the velocities \dot{X} , \dot{Y} and \dot{Z} are negligible with respect to their
138 values in the slipping modes. Therefore the region of phase space including
139 the states in which the asperities are stationary (sticking region) is a subset
140 of the space XYZ . It is the region bounded by the planes $X = 0$, $Y = 0$, Π_1
141 and Π_2 : a tetrahedron \mathbf{T} (Fig. 2).

142 A seismic event takes place when the orbit of the system reaches one of
143 the faces ACD or BCD of \mathbf{T} , belonging respectively to the planes Π_1 and Π_2 .
144 In these cases, the system passes from mode 00 to mode 10 or 01 respectively.
145 If the orbit reaches the edge CD , the system passes instead to mode 11. For
146 later use, we introduce a point P with coordinates

$$X_P = \frac{\alpha + \alpha\beta + 1}{1 + 2\alpha}, \quad Y_P = \frac{\alpha + \alpha\beta + \beta}{1 + 2\alpha}, \quad Z_P = -\frac{1 - \beta}{1 + 2\alpha} \quad (10)$$

147 It belongs to the edge CD and corresponds to the case of elastic coupling:
148 in fact $Z_P = Y_P - X_P$.

149 **3 Equations of motion and solutions**

150 The equations of motions of the four dynamic modes and the corresponding
151 solutions are given below. Viscoelastic relaxation is negligible during the
152 slipping modes: therefore the equations for X and Y are the same as in
153 the case of elastic coupling, while Z changes according to the equation $\ddot{Z} =$
154 $\ddot{Y} - \ddot{X}$.

155 **3.1 Stationary asperities (mode 00)**

156 The variables X and Y increase steadily due to tectonic motions, while Z is
157 governed by the Maxwell constitutive equation. The equations of motion are

$$\ddot{X} = 0, \quad \ddot{Y} = 0, \quad \ddot{Z} = \frac{Z}{\Theta^2} \quad (11)$$

158 where a dot indicates differentiation with respect to T . The fault can enter
159 mode 00 from mode 10 or from mode 01. With initial conditions

$$X(0) = \bar{X}, \quad Y(0) = \bar{Y}, \quad Z(0) = \bar{Z} \quad (12)$$

160

$$\dot{X}(0) = V, \quad \dot{Y}(0) = V, \quad \dot{Z}(0) = -\frac{\bar{Z}}{\Theta} \quad (13)$$

161 the solution is

$$X(T) = \bar{X} + VT, \quad Y(T) = \bar{Y} + VT, \quad Z(T) = \bar{Z}e^{-T/\Theta} \quad (14)$$

162 with $T \geq 0$. The initial point belongs necessarily to \mathbf{T} and (14) are the
163 parametric equations of a curve lying on the plane

$$X - Y + \bar{Y} - \bar{X} = 0 \quad (15)$$

164 which is parallel to the Z axis.

165 **3.2 Failure of asperity 1 (mode 10)**

166 The equations of motion are

$$\ddot{X} + X - \alpha Z - \epsilon = 0 \quad (16)$$

$$\ddot{Y} = 0 \quad (17)$$

$$\ddot{Z} - X + \alpha Z + \epsilon = 0 \quad (18)$$

167 The fault can enter mode 10 from mode 11 or from mode 00.

168 a) *Case 11* \rightarrow 10. With initial conditions

$$X(0) = \bar{X}, \quad Y(0) = \bar{Y}, \quad Z(0) = \bar{Z} \quad (19)$$

169

$$\dot{X}(0) = \bar{V}, \quad \dot{Y}(0) = 0, \quad \dot{Z}(0) = -\bar{V} \quad (20)$$

170 the solution is

$$X(T) = \bar{X} - \frac{\bar{U}_1}{2}(1 - \cos \omega T) + \frac{\bar{V}}{\omega} \sin \omega T \quad (21)$$

$$Y(T) = \bar{Y} \quad (22)$$

$$Z(T) = \bar{Z} + \bar{X} - X(T) \quad (23)$$

171 where

$$\bar{U}_1 = 2 \frac{\bar{X} - \alpha \bar{Z} - \epsilon}{\omega^2} \quad (24)$$

172 The slip duration, calculated from the condition $\dot{X}(T) = 0$, is

$$T_{10} = \frac{1}{\omega} \left(\pi + \arctan \frac{2\bar{V}}{\omega \bar{U}_1} \right) \quad (25)$$

173 and the final slip amplitude is

$$U_{10} = \frac{\bar{U}_1}{2} + \sqrt{\left(\frac{\bar{U}_1}{2}\right)^2 + \left(\frac{\bar{V}}{\omega}\right)^2} \quad (26)$$

174 *b) Case 00* \rightarrow 10. In this case the initial point belongs to the face *ACD* so
 175 that

$$\bar{X} - \alpha\bar{Z} = 1, \quad \bar{V} = 0 \quad (27)$$

176 and from (24)

$$\bar{U}_1 = U \quad (28)$$

177 The solution reduces to

$$X(T) = \bar{X} - \frac{U}{2}(1 - \cos \omega T) \quad (29)$$

$$Y(T) = \bar{Y} \quad (30)$$

$$Z(T) = \bar{Z} + \frac{U}{2}(1 - \cos \omega T) \quad (31)$$

178 If the orbit does not reach the face *BCD* during the mode, one has

$$T_{10} = \frac{\pi}{\omega}, \quad U_{10} = U \quad (32)$$

179 If the orbit reaches *BCD* before time π/ω has elapsed, the system passes to
 180 mode 11. In this case,

$$T_{10} = \frac{\pi}{\omega} - \frac{1}{\omega} \arccos\left(2\frac{U_{10}}{U} - 1\right) \quad (33)$$

181 where

$$U_{10} = \frac{\beta - \bar{Y} - \alpha\bar{Z}}{\alpha} \quad (34)$$

182 **3.3 Failure of asperity 2 (mode 01)**

183 The equations of motion are

$$\ddot{X} = 0 \quad (35)$$

$$\ddot{Y} + Y + \alpha Z - \beta\epsilon = 0 \quad (36)$$

$$\ddot{Z} + Y + \alpha Z - \beta\epsilon = 0 \quad (37)$$

184 The fault can enter mode 01 from mode 11 or from mode 00.

185 a) *Case* 11 \rightarrow 01. With initial conditions

$$X(0) = \bar{X}, \quad Y(0) = \bar{Y}, \quad Z(0) = \bar{Z} \quad (38)$$

186

$$\dot{X}(0) = 0, \quad \dot{Y}(0) = \bar{V}, \quad \dot{Z}(0) = \bar{V} \quad (39)$$

187 the solution is

$$X(T) = \bar{X} \quad (40)$$

$$Y(T) = \bar{Y} - \frac{\bar{U}_2}{2}(1 - \cos \omega T) + \frac{\bar{V}}{\omega} \sin \omega T \quad (41)$$

$$Z(T) = \bar{Z} - \bar{Y} + Y(T) \quad (42)$$

188 where

$$\bar{U}_2 = 2 \frac{\bar{Y} + \alpha \bar{Z} - \beta \epsilon}{\omega^2} \quad (43)$$

189 The slip duration, calculated from the condition $\dot{Y}(T) = 0$, is

$$T_{01} = \frac{1}{\omega} \left(\pi + \arctan \frac{2\bar{V}}{\omega \bar{U}_2} \right) \quad (44)$$

190 and the final slip amplitude is

$$U_{01} = \frac{\bar{U}_2}{2} + \sqrt{\left(\frac{\bar{U}_2}{2} \right)^2 + \left(\frac{\bar{V}}{\omega} \right)^2} \quad (45)$$

191 b) *Case* 00 \rightarrow 01. In this case the initial point belongs to the face *BCD* so

192 that

$$\bar{Y} + \alpha \bar{Z} = \beta, \quad \bar{V} = 0 \quad (46)$$

193 and from (43)

$$\bar{U}_2 = \beta U \quad (47)$$

194 The solution reduces to

$$X(T) = \bar{X} \quad (48)$$

$$Y(T) = \bar{Y} - \frac{\beta U}{2}(1 - \cos \omega T) \quad (49)$$

$$Z(T) = \bar{Z} - \frac{\beta U}{2}(1 - \cos \omega T) \quad (50)$$

195 If the orbit does not reach the face ACD during the mode, one has

$$T_{01} = \frac{\pi}{\omega}, \quad U_{01} = \beta U \quad (51)$$

196 If the orbit reaches ACD before time π/ω has elapsed, the system passes to
197 mode 11. In this case,

$$T_{01} = \frac{\pi}{\omega} - \frac{1}{\omega} \arccos\left(2\frac{U_{01}}{\beta U} - 1\right) \quad (52)$$

198 where

$$U_{01} = \frac{1 - \bar{X} + \alpha \bar{Z}}{\alpha} \quad (53)$$

199 **3.4 Simultaneous asperity failure (mode 11)**

200 The equations of motion are

$$\ddot{X} + X - \alpha Z - \epsilon = 0 \quad (54)$$

$$\ddot{Y} + Y + \alpha Z - \beta \epsilon = 0 \quad (55)$$

$$\ddot{Z} - X + Y + 2\alpha Z + (1 - \beta)\epsilon = 0 \quad (56)$$

201 and the solution is

$$X(T) = A \sin T + B \cos T + C \sin \Omega T + D \cos \Omega T + E_1 \quad (57)$$

$$Y(T) = A \sin T + B \cos T - C \sin \Omega T - D \cos \Omega T + E_2 \quad (58)$$

$$Z(T) = -2C \sin \Omega T - 2D \cos \Omega T + E_3 \quad (59)$$

202 where the constants $A, B, C, D, E_1, E_2, E_3$ depend on initial conditions.

203 The fault can enter mode 11 from mode 10, 01 or 00.

204 a) *Case* 10 \rightarrow 11. The initial conditions are

$$X = \bar{X}, \quad Y = \bar{Y}, \quad Z = \bar{Z} \quad (60)$$

205

$$\dot{X} = \bar{V}, \quad \dot{Y} = 0, \quad \dot{Z} = -\bar{V} \quad (61)$$

206 and the constants are

$$B = \frac{1}{2}[\bar{X} + \bar{Y} - \epsilon(X_P + Y_P)] \quad (62)$$

$$D = \frac{1}{2} \left(\epsilon Z_P + \frac{\bar{X} - \bar{Y} - 2\alpha\bar{Z}}{\Omega^2} \right) \quad (63)$$

$$E_1 = \epsilon X_P + \alpha \frac{\bar{X} - \bar{Y} + \bar{Z}}{\Omega^2} \quad (64)$$

$$E_2 = \epsilon Y_P - \alpha \frac{\bar{X} - \bar{Y} + \bar{Z}}{\Omega^2} \quad (65)$$

$$E_3 = \epsilon Z_P + \frac{\bar{X} - \bar{Y} + \bar{Z}}{\Omega^2} \quad (66)$$

$$A = \frac{\bar{V}}{2}, \quad C = \frac{\bar{V}}{2\Omega} \quad (67)$$

207 b) *Case* 01 \rightarrow 11. The initial conditions are

$$X = \bar{X}, \quad Y = \bar{Y}, \quad Z = \bar{Z} \quad (68)$$

208

$$\dot{X} = 0, \quad \dot{Y} = \bar{V}, \quad \dot{Z} = \bar{V} \quad (69)$$

209 The constants B, D, E_1, E_2, E_3 are given by (62)-(66), while

$$A = \frac{\bar{V}}{2}, \quad C = -\frac{\bar{V}}{2\Omega} \quad (70)$$

210 c) *Case* 00 \rightarrow 11. The initial conditions are

$$X = \bar{X}, \quad Y = \bar{Y}, \quad Z = \bar{Z} \quad (71)$$

211

$$\dot{X} = 0, \quad \dot{Y} = 0, \quad \dot{Z} = 0 \quad (72)$$

212 The constants B, D, E_1, E_2, E_3 are given by (62)-(66), while

$$A = 0, \quad C = 0 \quad (73)$$

213

4 The sequence of slipping modes

214 In general, a seismic event will involve n slipping modes of the fault. The
 215 sequence of slipping modes determines not only the source function and the
 216 seismic moment of the earthquake, but also the position of its focus. We wish
 217 to find the relationship between the state of the fault before the earthquake
 218 and the sequence of slipping modes.

219 During the interseismic intervals, the fault is subject to continuous tec-
 220 tonic loading due to the motion of adjacent plates and to the effect of vis-
 221 coelastic relaxation of the stress accumulated by previous seismic activity.
 222 Given any state $P_0 = (X_0, Y_0, Z_0) \in \mathbf{T}$, its orbit will lead to the failure of
 223 asperity 1 or asperity 2 or to the simultaneous failure of both asperities. In
 224 fact, all the orbits (14) in mode 00 reach one of the faces ACD or BCD or
 225 their common edge CD . We wish to determine the subset \mathbf{T}_1 of the sticking
 226 region \mathbf{T} such that, if $P_0 \in \mathbf{T}_1$, the orbit reaches ACD and the subset \mathbf{T}_2
 227 such that, if $P_0 \in \mathbf{T}_2$, the orbit reaches BCD .

228 Any curve (14), if prolonged outside \mathbf{T} , intersects both Π_1 and Π_2 . Let
 229 $P_1 = (X_1, Y_1, Z_1)$ and $P_2 = (X_2, Y_2, Z_2)$ be the intersection points with the
 230 two planes respectively and let T_1 and T_2 be the corresponding instants of

231 time. Accordingly, X_1 and Z_1 must satisfy (8) or, thanks to (14),

$$X_0 + VT_1 = 1 + \alpha Z_0 e^{-T_1/\Theta} \quad (74)$$

232 whence

$$T_1 = \Theta W(\gamma_1) + \frac{1 - X_0}{V} \quad (75)$$

233 where W is the Lambert function with argument

$$\gamma_1 = \frac{\alpha Z_0}{V\Theta} e^{-\frac{1-X_0}{V\Theta}} \quad (76)$$

234 Analogously, Y_2 and Z_2 must satisfy (9) or, thanks to (14),

$$Y_0 + VT_2 = \beta - \alpha Z_0 e^{-T_2/\Theta} \quad (77)$$

235 whence

$$T_2 = \Theta W(\gamma_2) + \frac{\beta - Y_0}{V} \quad (78)$$

236 with

$$\gamma_2 = -\frac{\alpha Z_0}{V\Theta} e^{-\frac{\beta-Y_0}{V\Theta}} \quad (79)$$

237 We consider the difference

$$\Delta T = T_1 - T_2 \quad (80)$$

238 and define a surface Σ with the equation

$$\Delta T(X, Y, Z) = 0 \quad (81)$$

239 or, thanks to (75) and (78),

$$V\Theta [W(\gamma_1) - W(\gamma_2)] + Y - X + 1 - \beta = 0 \quad (82)$$

240 This is a transcendental surface that divides \mathbf{T} in two connected, open subsets
 241 \mathbf{T}_1 and \mathbf{T}_2 with the required properties (Fig. 3). If $\beta = 1$, the surface Σ
 242 divides \mathbf{T} in two halves; if $\beta < 1$, \mathbf{T}_1 has a smaller volume than \mathbf{T}_2 . The
 243 edge CD of \mathbf{T} belongs to Σ . By definition, no orbit can cross Σ : therefore,
 244 if $P_0 \in \Sigma$, its orbit remains on Σ and reaches the edge CD .

245 After an orbit reaches one of the faces ACD or BCD at a point P_k , the
 246 sequence of modes in the earthquake will be different according to which
 247 subset of the face P_k belongs to. This is illustrated in Fig. 4. Let us consider
 248 the face ACD . If P_k belongs to the triangle Q_1 , the earthquake will be a
 249 1-mode event 10. If P_k belongs to the segment s_1 , the earthquake will be a
 250 2-mode event 10-01. If P_k belongs to the trapezoid R_1 , the earthquake will be
 251 a 3-mode event 10-11-10 or 10-11-01. The remaining part of the face would
 252 lead to overshooting. Analogous considerations can be made for subsets Q_2 ,
 253 s_2 and R_2 of the face BCD .

254 Therefore, events involving the simultaneous failure of asperities can take
 255 place only from particular subsets of states of the system. In general, a
 256 3-mode event can result from four different sequences of modes: 10-11-10,
 257 10-11-01, 01-11-10, 01-11-01. In particular cases, sequences like 10-01-10 or
 258 01-10-01 are also possible.

259 The reasons for the different sequences of modes involved in the earth-
 260 quake are clear if we consider the forces acting on the asperities in the differ-
 261 ent states. If we consider the face ACD , we have $F_1 = -1$ everywhere, while
 262 F_2 is equal to $-\beta$ on CD and decreases in magnitude with the distance from
 263 this edge. Hence, the onset mode 10 of the sequence can trigger mode 11

264 only if $|F_2|$ is large enough and this occurs if $P_k \in R_1$. When $F_2 = -(\beta - \alpha U)$
 265 we have the limit case of two consecutive modes 10-01. For smaller values
 266 of $|F_2|$, no triggering occurs and the earthquake is a 1-mode event 10. The
 267 same considerations can be made for the face BCD .

268 This analysis enlightens the relationship between the state of the fault
 269 before an earthquake and the sequence of modes in the seismic event. It also
 270 suggests that the knowledge of the source function of an earthquake may
 271 allow us to constrain the orbit of the system in the phase space.

272 5 Seismic moment rates

273 The number and the sequence of slipping modes involved in a seismic event
 274 determine the moment rate of the earthquake. Let P_i be the singular points of
 275 the orbit, i.e. the points where the system passes from one mode to another.
 276 If the seismic event begins at P_k , the representative point of the system when
 277 it enters the i -th slipping mode is P_{k+i-1} and the corresponding instant of
 278 time is T_{k+i-1} ($i = 1, 2, \dots, n$). The duration of the i -th mode is

$$\Delta T_i = T_{k+i} - T_{k+i-1} \quad (83)$$

279 and the seismic event terminates at time T_{k+n} . In the i -th mode, the slip
 280 functions of asperities 1 and 2 are respectively

$$\Delta X_i(T) = X_{k+i-1} - X(T - T_{k+i-1}) \quad (84)$$

281

$$\Delta Y_i(T) = Y_{k+i-1} - Y(T - T_{k+i-1}) \quad (85)$$

282 where the appropriate expressions of $X(T)$ and $Y(T)$ must be used. The
 283 moment rate of an n -mode seismic event can be calculated as

$$\dot{M}(T) = \frac{M_1}{U} \sum_{i=1}^n (\Delta \dot{X}_i + \Delta \dot{Y}_i) [H(T - T_{k+i-1}) - H(T - T_{k+i})] \quad (86)$$

284 where M_1 is the seismic moment due to the slip of asperity 1 by an amount
 285 U and $H(T)$ is the Heaviside function. The final slip amplitudes of asperities
 286 1 and 2 are respectively

$$U_1 = \sum_{i=1}^n \Delta X_i(T_{k+i}), \quad U_2 = \sum_{i=1}^n \Delta Y_i(T_{k+i}) \quad (87)$$

287 and the final seismic moment is

$$M_0 = M_1 \frac{U_1 + U_2}{U} \quad (88)$$

288 The moment rate depends on the state of the fault at the beginning of the
 289 seismic event, i.e. on the coordinates X_k , Y_k and Z_k . This state is a priori
 290 unknown, but the knowledge of the source function of the earthquake allows
 291 us to set constraints on it. As shown in section 4, if the first mode is 10 or
 292 01, P_k must belong to the face ACD or BCD of \mathbf{T} . In addition, if the event
 293 has a single mode, P_k belongs to the subset Q_1 or Q_2 ; if the event has two
 294 modes, P_k belongs to the segment s_1 or s_2 ; if the event has three modes, P_k
 295 belongs to the subset R_1 or R_2 .

296 This allows us to constrain the evolution of the system to a certain subset
 297 of the phase space and, when the next earthquake will occur, the knowledge
 298 of its moment rate will allow us to further constrain this subset. Hence, if
 299 we knew the source functions of a sufficiently large number of consecutive
 300 earthquakes, we could constrain more and more the orbit of the system and
 301 its evolution could be predicted with a smaller uncertainty.

302 **6 Application to the 1964 Alaska earthquake**

303 The 1964 Alaska earthquake was one of the largest earthquakes in the last
304 century, with a seismic moment $M_0 = 3 \times 10^{22}$ Nm (Christensen and Beck,
305 1994; Holdahl and Sauber, 1994; Johnson et al., 1996; Ichinose et al., 2007).
306 Seismological, geodetic and tsunami data indicate that the earthquake was
307 the result of the slipping of two asperities, the Prince William Sound and
308 the Kodiak Island asperity, that we call asperity 1 and 2 respectively. The
309 earthquake started with the failure of asperity 1 followed by that of asperity 2.
310 On the basis of coseismic surface deformation, Santini et al. (2003) suggested
311 average slips $u_1 = 24$ m for asperity 1 and $u_2 = 18$ m for asperity 2.

312 For the Alaska earthquake there is clear evidence of post-seismic defor-
313 mation occurred in the decades following the event (Zweck et al., 2002; Suito
314 and Freymueller, 2009). Part of the deformation has been ascribed to aseis-
315 mic slip of the fault and part to viscoelastic relaxation. The latter shows
316 a characteristic time $\tau \approx 30$ a. The relative plate velocity is $v = 5.7$ cm
317 a^{-1} (DeMets and Dixon, 1999; Cohen and Freymueller, 2004). In fact, the
318 velocity of the Pacific Plate relative to the North American Plate at the
319 Alaska/Aleutian Trench increases gradually from the northeast to the south-
320 west. However, the difference between the area of Prince William Sound and
321 the area of Kodiak Island is small, in the order of few mm per year, and can
322 be reasonably neglected.

323 According to the present model, the seismic event was a sequence of
324 modes 10-01 starting from mode 00. Since the first mode was 10, the orbit of
325 the system in mode 00 was in the subset \mathbf{T}_1 of the sticking region. Let P_1 be

326 the representative point of the system at the beginning of the seismic event.
 327 Since mode 10 was followed by mode 01, P_1 belongs to segment s_1 (Fig. 4).
 328 We may express the coordinates of P_1 as

$$X_1 = \alpha Z_1 + 1, \quad Y_1 = \beta - \alpha U - \alpha Z_1, \quad Z_1 \quad (89)$$

329 with

$$Z_a \leq Z_1 \leq Z_b \quad (90)$$

330 where

$$Z_a = -\frac{1-U}{\alpha}, \quad Z_b = \frac{\beta - (\alpha + \beta)U}{\alpha} \quad (91)$$

331 The orbit of the system is one of the bundle of curves with parametric equa-
 332 tions (14) passing through s_1 . At the end of mode 10, the system is at P_2
 333 with coordinates

$$X_2 = \alpha Z_1 + 1 - U, \quad Y_2 = \beta - \alpha U - \alpha Z_1, \quad Z_2 = Z_1 + U \quad (92)$$

334 As Z_1 varies in the interval (90), there is an infinite number of points P_2
 335 forming another segment r_1 belonging to the face BCD and parallel to the
 336 edge CD . At the end of the event, the system is at P_3 , with coordinates

$$X_3 = \alpha Z_1 + 1 - U, \quad Y_3 = \beta - (\alpha + \beta)U - \alpha Z_1, \quad Z_3 = Z_1 + (1 - \beta)U \quad (93)$$

337 As Z_1 varies in the interval (90), there is an infinite number of points P_3
 338 forming another segment q_1 . This segment is also parallel to the edge CD .
 339 However it intersects the surface Σ for $Z_1 = Z_c$, with $Z_a < Z_c < Z_b$.

340 From (1), it is easy to calculate the forces on the asperities at points P_1 ,
 341 P_2 and P_3 . These forces are independent of the positions of the points on

342 the respective segments s_1 , r_1 and q_1 :

$$F_1 = -1, \quad F_2 = -(\beta - \alpha U) \quad \text{on } s_1 \quad (94)$$

$$F_1 = -(2\epsilon - 1), \quad F_2 = -\beta \quad \text{on } r_1 \quad (95)$$

$$F_1 = -(2\epsilon - 1 + \alpha\beta U), \quad F_2 = -(2\epsilon - 1)\beta \quad \text{on } q_1 \quad (96)$$

343 For an application of the model to the Alaska earthquake, we take $\alpha = 0.1$,
 344 $\beta = 0.75$, $\epsilon = 0.7$ (Dragoni and Santini, 2012). It follows $U \simeq 0.545$ and
 345 $V\Theta \simeq 0.039$. With these values, (91) yields $Z_a \simeq -4.55$ and $Z_b \simeq 2.86$, while
 346 $Z_c \simeq 0.41$.

347 Then, according to (94)-(96), the forces immediately before the 1964
 348 earthquake are $F_1(T_1) = -1$ and $F_2(T_1) = -0.70$, showing that the mag-
 349 nitude of stress on asperity 2 is 70% of that on asperity 1. The failure of
 350 asperity 1 reduces the stress on asperity 1 and transfers stress to asperity 2
 351 up to static friction, so that $F_1(T_2) = -0.40$ and $F_2(T_2) = -0.75$. Finally, the
 352 failure of asperity 2 reduces the stress on asperity 2 and transfers stress back
 353 to asperity 1, so that at the end of the event it results $F_1(T_3) = -0.44$ and
 354 $F_2(T_3) = -0.30$, indicating a more homogeneous stress distribution. Then
 355 the system evolves in mode 00, where both stresses increase in magnitude,
 356 but at different rates.

357 7 Post-seismic evolution

358 On the basis of a purely elastic model, Dragoni and Santini (2012) predicted
 359 that the next large earthquake involving the 1964 fault would take place
 360 about 350 years later and would be due to the failure of asperity 2 alone. If

361 we introduce viscoelastic relaxation, a wider range of possibilities appears.
 362 Since the segment q_1 intersects Σ , the point P_3 can belong to \mathbf{T}_1 , \mathbf{T}_2 or
 363 Σ . In the first case, the next event will start with the failure of asperity 1,
 364 in the second case with the failure of asperity 2, in the third case with the
 365 simultaneous failure of both asperities.

366 According to the present model, the duration of the interseismic interval
 367 between 1964 and the next earthquake is

$$\frac{T'}{\Theta} = \begin{cases} W(\gamma'_1) + \frac{1 - X_3}{V\Theta}, & P_3 \in \mathbf{T}_1 \\ W(\gamma'_2) + \frac{\beta - Y_3}{V\Theta}, & P_3 \in \mathbf{T}_2 \end{cases} \quad (97)$$

368 where

$$\gamma'_1 = \frac{\alpha Z_3}{V\Theta} e^{-\frac{1-X_3}{V\Theta}}, \quad \gamma'_2 = -\frac{\alpha Z_3}{V\Theta} e^{-\frac{\beta-Y_3}{V\Theta}} \quad (98)$$

369 Thanks to (93), the coordinates of P_3 can be expressed as functions of Z_1 .
 370 The function $T'/\Theta(Z_1)$ is shown in Fig. 5a. The duration of the interseismic
 371 interval ranges from about 2 to 13 Θ , that is from about 60 to 390 a. The
 372 maximum value is obtained for $Z_1 = Z_c$. We conclude that the evolution
 373 of the system after the 1964 event depends on the particular state P_1 from
 374 which the 1964 event was originated. Since we have expressed X_1 and Y_1 as
 375 functions of Z_1 , we may characterize the evolution by the value of Z_1 as well.

376 In general, the next event will be an n -mode event beginning at a point
 377 P_4 with coordinates

$$X_4 = X_3 + VT', \quad Y_4 = Y_3 + VT', \quad Z_4 = Z_3 e^{-T'/\Theta} \quad (99)$$

378 where T' is given by (97). There is an infinite number of possible points P_4
 379 belonging in part to face ACD , in part to BCD . Thanks to (1), (93) and

380 (99), the forces at P_4 are

$$F_1(T_4) = -\alpha Z_1 - 1 + U - VT' + \alpha[Z_1 + (1 - \beta)U] e^{-T'/\Theta} \quad (100)$$

381

$$F_2(T_4) = \alpha Z_1 - \beta + (\alpha + \beta)U - VT' - \alpha[Z_1 + (1 - \beta)U] e^{-T'/\Theta} \quad (101)$$

382 In contrast with the forces (96) at P_3 , they depend on the particular point
 383 P_4 , hence on Z_1 (Fig. 5b), a consequence of viscoelastic relaxation during
 384 the interseismic interval.

385 Hence the interval $[Z_a, Z_b]$ can be divided into subintervals leading to
 386 different evolutions. If $-4.55 \leq Z_1 < 0.20$ the next earthquake will be a
 387 1-mode event 01. If $0.20 \leq Z_1 < 0.41$, it will be a 3-mode event 01-11-10. If
 388 $Z_1 = 0.41$, it will be a 2-mode event 11-10. If $0.41 < Z_1 < 0.70$, it will be
 389 a 3-mode event 10-11-10. Finally, if $0.70 \leq Z_1 \leq 2.86$, it will be a 1-mode
 390 event 10.

391 The corresponding values of the seismic moment M_0 calculated from (88)
 392 are shown in Fig. 5c and compared with the moment of the 1964 earthquake.
 393 It can be seen that the occurrence of an event with a moment greater than
 394 the 1964 one is possible only if the value of Z_1 is in a narrow range, entailing
 395 a narrow range of possible stress distributions on the fault.

396 Examples of moment rates \dot{M} for the next great Alaska earthquake are
 397 shown in Fig. 6 for different values of Z_1 . The graphs show moment rates
 398 for 1-mode events 01 (Fig. 6a) and 10 (6e), for a 2-mode event 11-10 (6c),
 399 and for 3-mode events 01-11-10 (6b) and 10-11-10 (6d).

400 8 Conclusions

401 We considered a fault with two asperities of different strengths, placed in a
402 shear zone subject to a constant strain rate by the motion of adjacent tectonic
403 plates. The equations of motion were written under the hypothesis that the
404 asperities have the same area: this is a reasonable approximation for many
405 earthquakes. The system has been represented by a discrete model described
406 by three variables: the slip deficits of the asperities and the viscoelastic
407 deformation. The system dynamics has one sticking mode and three slipping
408 modes, for which we solved analytically the equations of motion.

409 If the state of the fault at a given instant of time is known in terms of
410 the system variables, we can calculate the orbit of the system in the phase
411 space and hence predict its evolution. The state of a fault is not directly
412 measurable, but the model shows that the knowledge of the earthquake source
413 functions allows us to constrain the orbit of the system.

414 The study of the sticking region of the phase space shows how the state of
415 the system before a seismic event controls the sequence of slipping modes in
416 the event. Since the moment rate depends on the number and the sequence
417 of slipping modes, the knowledge of the source function of an earthquake
418 constrains the possible states of the system, hence its orbit in the phase
419 space. Then, if we knew the source functions of a sufficiently large number
420 of consecutive earthquakes, we could constrain the orbit more and more and
421 predict its evolution with a smaller uncertainty.

422 As an example, we considered the fault that originated the 1964 Alaska
423 earthquake. This earthquake was due to the failure of two distinct asperities;

424 being a large-size event, it was followed by remarkable post-seismic deforma-
425 tion; in addition, more than 50 years have elapsed since the earthquake,
426 allowing such a deformation to be observed over a sufficiently long period
427 of time. The knowledge of the source function of this earthquake allows us
428 to determine the subset of phase space in which the system was before 1964
429 and the subset to which it came afterwards. This constrains the evolution of
430 the system to a certain bundle of orbits in the phase space, but still allows
431 a wide range of possible occurrence times and source functions for the next
432 earthquake. However, when the next earthquake will occur, the knowledge
433 of its moment rate will allow us to further constrain the orbit, and so on.

434 The present model is of course a simplification of a real fault, but it
435 suggests how the accumulation of knowledge on the seismic activity of a
436 fault may allow us to constrain the state of the fault and to predict its future
437 activity.

438 *Acknowledgments*

439 The authors are grateful to the editor Ilya Zaliapin, to J. Freymueller and to
440 an anonymous referee for useful comments on the first version of the paper.

441 **References**

442 Amendola, A., and Dragoni, M.: Dynamics of a two-fault system with
443 viscoelastic coupling, *Nonlin. Processes Geophys.*, 20, 1–10, doi: 10.5194/
444 npg-20-1-2013, 2013.

445 Bürgmann, R. and Dresen, G.: Rheology of the lower crust and upper

446 mantle: evidence from rock mechanics, geodesy, and field observation,
447 *Ann. Rev. Earth Planet. Sci.*, 36, 531–567, 2008.

448 Carter, N.L.: Steady state flow of rocks, *Rev. Geophys. Space Phys.*, 14,
449 301–353, 1976.

450 Christensen, D.H. and Beck, S.L.: The rupture process and tectonic im-
451 plications of the great 1964 Prince William Sound earthquake, *Pure Appl.*
452 *Geophys.*, 142, 29-53, 1994.

453 Cohen, S.C. and Freymueller, J.T.: Crustal Deformation in the Southcen-
454 tral Alaska Subduction Zone, *Advances in Geophysics*, 47, 1-63, 2004.

455 Delouis, B., Nocquet, J.-M. and Vallée M.: Slip distribution of the Febru-
456 ary 27, 2010 Mw = 8.8 Maule earthquake, central Chile, from static and
457 high-rate GPS, InSAR, and broadband teleseismic data, *Geophys. Res.*
458 *Lett.*, 37, L17305, doi:10.1029/2010GL043899, 2010.

459 DeMets, C. and Dixon, T.H.: New kinematic models for Pacific-North
460 America motion from 3 Ma to present. Part 1. Evidence for steady motion
461 and biases in the NUVEL1-A model. *Geophys. Res. Lett.* 26, 1921-1924,
462 1999.

463 Dieterich, J.: A constitutive law for rate of earthquake production and
464 its application to earthquake clustering, *J. Geophys. Res.*, 99, 2601-2618,
465 1994. Ding, M. and Lin, J.: Post-seismic viscoelastic deformation and
466 stress transfer after the 1960 M9.5 Valdivia, Chile earthquake: effects on
467 the 2010 M8.8 Maule, Chile earthquake, *Geophys. J. Int.*, 2, 697–704, doi:
468 10.1093/gji/ggu048, 2014.

469 Dragoni, M. and Santini, S.: Long-term dynamics of a fault with two

470 asperities of different strengths, *Geophys. J. Int.*, 191, 1457-1467, doi:
471 10.1111/j.1365-246X.2012.05701.x, 2012.

472 Dragoni, M. and Santini, S.: Source functions of a two-asperity fault
473 model, *Geophys. J. Int.*, 196, 1803-1812, doi: 10.1093/gji/ggt491, 2014.

474 Holdahl, S. and Sauber, J.: Coseismic slip in the 1964 Prince William
475 Sound earthquake: a new geodetic inversion, *Pure Appl. Geophys.*, 142,
476 55-82, 1994.

477 Huang, J. and Turcotte, D. L.: Are earthquakes an example of determin-
478 istic chaos?, *Geophys. Res. Lett.*, 17, 223-226, 1990.

479 Huang, J. and Turcotte, D. L.: Chaotic seismic faulting with mass-spring
480 model and velocity-weakening friction, *Pure Appl. Geophys.*, 138, 569-589,
481 1992.

482 Ichinose, G., Somerville, P., Thio, H.K., Graves, R. and O'Connell, D.:
483 Rupture process of the 1964 Prince William Sound, Alaska, earthquake
484 from the combined inversion of seismic, tsunami, and geodetic data, *J.*
485 *Geophys. Res.*, 112, B07306, doi:10.1029/2006JB004728, 2007.

486 Johanson, I.A., Fielding, E.J., Rolandone, F. and Bürgmann, R.: Coseis-
487 mic and postseismic slip of the 2004 Parkfield earthquake from space-
488 geodetic data, *Bull. Seismol. Soc. Am.*, 96, S269-S282, doi: 10.1785/
489 0120050818, 2006.

490 Johnson, J.M., Satake, K., Holdahl, S.H. and Sauber, J.: The 1964 Prince
491 William Sound earthquake: joint inversion of tsunami and geodetic data,
492 *J. Geophys. Res.*, 101, 523-532, 1996.

493 Kenner, S., and Segall, P.: Postseismic deformation following the 1906 San

494 Francisco earthquake, *J. Geophys. Res.*, 105(B6), 13195–13209, 2000.

495 Kikuchi, M. and Kanamori, H.: Rupture Process of the Kobe, Japan, of
496 Jan. 17, 1995, determined from teleseismic body waves, *J. Phys. Earth*,
497 44, 429–436, 1996.

498 Kirby, S.H. and Kronenberg, A.K.: Rheology of the lithosphere: selected
499 topics, *Rev. Geophys.*, 25, 1219–1244, 1987.

500 Kuzsnir, N.J.: The distribution of stress with depth in the lithosphere:
501 thermo-rheological and geodynamic constraints, *Phil. Trans. R. Soc. Lond.*
502 A 337, 95–110, 1991.

503 Lay T., Kanamori, H. and Ruff, L.: The asperity model and the nature of
504 large subduction zone earthquakes, *Earthq. Pred. Res.*, 1, 3–71, 1982.

505 McCloskey, J. and Bean, C. J.: Time and magnitude predictions in shocks
506 due to chaotic fault interactions, *Geophys. Res. Lett.*, 19, 119–122, 1992.

507 Nishimura, T. and Thatcher, W.: Rheology of the lithosphere inferred from
508 postseismic uplift following the 1959 Hebgen Lake earthquake, *J. Geophys.*
509 *Res.*, 108, 2389, doi: 10:1029/2002JB002191, 2003.

510 Nussbaum, J. and Ruina, A.: A two degree-of-freedom earthquake model
511 with static/dynamic friction, *Pure Appl. Geophys.*, 125, 629–656, 1987.

512 Piombo A., Tallarico A., and Dragoni M.: Displacement, strain and stress
513 fields due to shear and tensile dislocations in a viscoelastic half-space, *Geo-*
514 *phys. J. Int.*, 170, 1399–1417, 2007.

515 Ranalli, G.: *Rheology of the Earth*, 2nd ed., Chapman & Hall, London,
516 1995.

517 Rice, J. R.: Spatio-temporal complexity of slip on a fault, *J. Geophys.*

518 Res., 98, 9885–9907, 1993.

519 Ruff, L. J.: Asperity distributions and large earthquake occurrence in sub-
520 duction zones, *Tectonophysics*, 211, 61–83, 1992.

521 Ruina, A.: Slip instability and state variable friction laws, *J. Geophys.*
522 *Res.*, 88, 10359-10370, 1983.

523 Santini, S., Dragoni, M. and Spada, G.: Asperity distribution of the 1964
524 great Alaska earthquake and its relation to subsequent seismicity in the
525 region, *Tectonophysics*, 367, 219–233, 2003.

526 Scholz, C. H.: *The Mechanics of Earthquakes and Faulting*, Cambridge
527 University Press, Cambridge, 1990.

528 Smith, B.R. and Sandwell, D.T.: A model of the earthquake cycle along
529 the San Andreas Fault System for the past 1000 years, *J. Geophys. Res.*,
530 111, B01405, doi:10.1029/2005JB003703, 2006.

531 Suito, H. and Freymueller, J.T.: A viscoelastic and afterslip postseismic
532 deformation model for the 1964 Alaska earthquake, *J. Geophys. Res.*, 114,
533 B11404, doi:10.1029/2008JB005954, 2009.

534 Turcotte, D. L.: *Fractals and Chaos in Geology and Geophysics*, 2nd edi-
535 tion, Cambridge University Press, Cambridge, 1997.

536 Zweck, C., Freymueller, J.T. and Cohen, S.C.: The 1964 great Alaska
537 earthquake: present day and cumulative postseismic deformation in the
538 western Kenai Peninsula, *Phys. Earth Planet. Int.*,, 132, 5-20, 2002.

539 **Figure captions**

540 Fig. 1 - The fault model. The state of the fault is described by the slip
541 deficits $X(T)$ and $Y(T)$ of the asperities and by the viscoelastic deformation
542 $Z(T)$.

543 Fig. 2 - The sticking region \mathbf{T} of the system is a tetrahedron $ABCD$ in the
544 phase space ($\alpha = 1, \beta = 1$). The point P is indicated.

545 Fig. 3 - The surface Σ divides the sticking region \mathbf{T} in two subsets \mathbf{T}_1 (below)
546 and \mathbf{T}_2 (above), which determine the first slipping mode of the seismic event
547 ($\alpha = 1, \beta = 1$).

548 Fig. 4 - The faces ACD and BCD of \mathbf{T} and their subsets, that determine
549 the sequence of slipping modes and the moment rate of the seismic event
550 ($\alpha = 1, \beta = 1, \epsilon = 0.7$).

551 Fig. 5 - (a) Duration T' of the interseismic interval following an event with
552 mode sequence 10-01; (b) forces F_1 and F_2 on the asperities at the beginning
553 of the subsequent event; and (c) seismic moment M_0 of the subsequent event,
554 as functions of the variable Z_1 characterizing the initial state of the system.
555 The values of parameters are appropriate to the 1964 Alaska earthquake
556 ($\alpha = 0.1, \beta = 0.75, \epsilon = 0.7, V\Theta = 0.039$).

557 Fig. 6 - Examples of possible moment rates $\dot{M}(T)$ for the event following
558 the 10-01 event: (a) $-4.55 \leq Z_1 < 0.20$; (b) $Z_1 = 0.30$; (c) $Z_1 = 0.41$; (d)
559 $Z_1 = 0.60$; (e) $0.70 \leq Z_1 \leq 2.86$, where Z_1 characterizes the initial state of
560 the system. The values of parameters are appropriate to the 1964 Alaska
561 earthquake ($\alpha = 0.1, \beta = 0.75, \epsilon = 0.7, V\Theta = 0.039$).

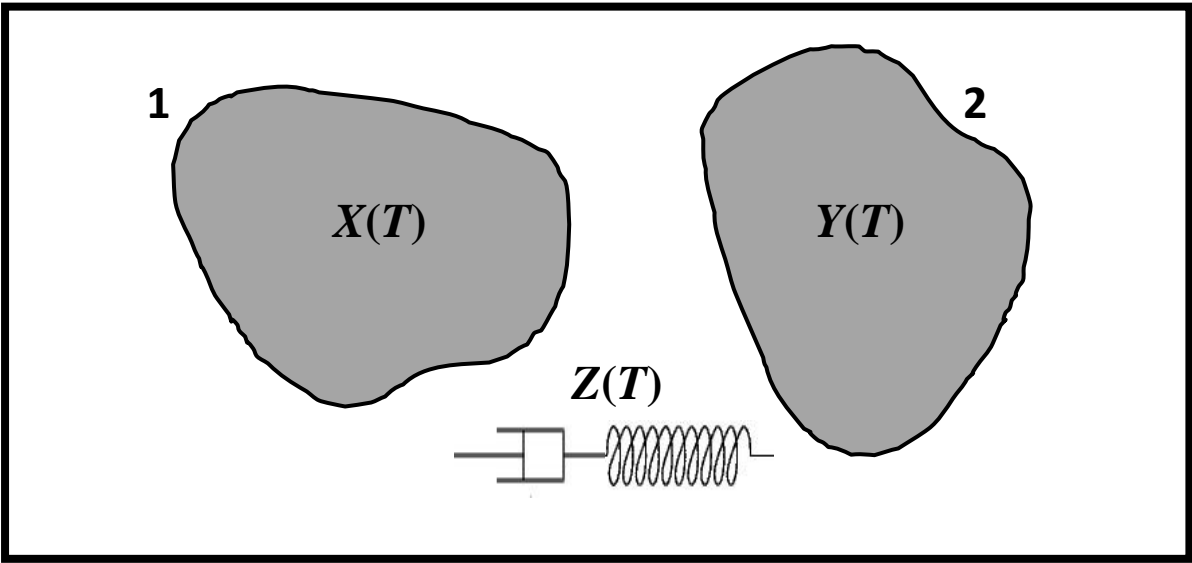


Fig. 1

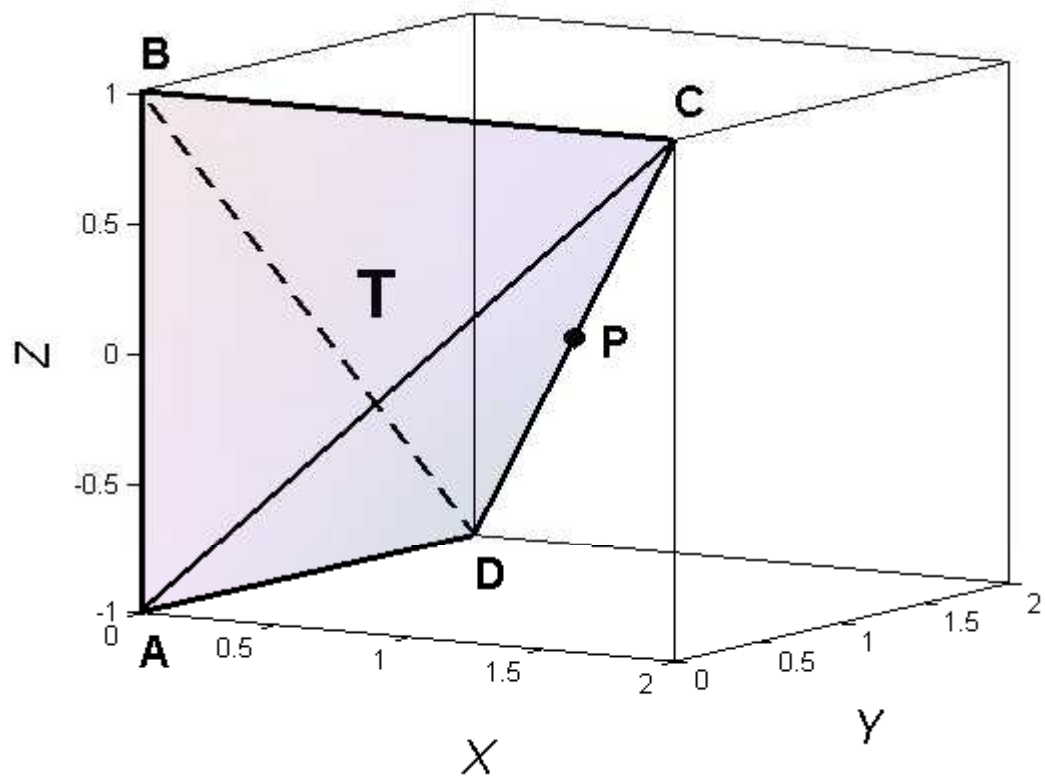


Fig. 2

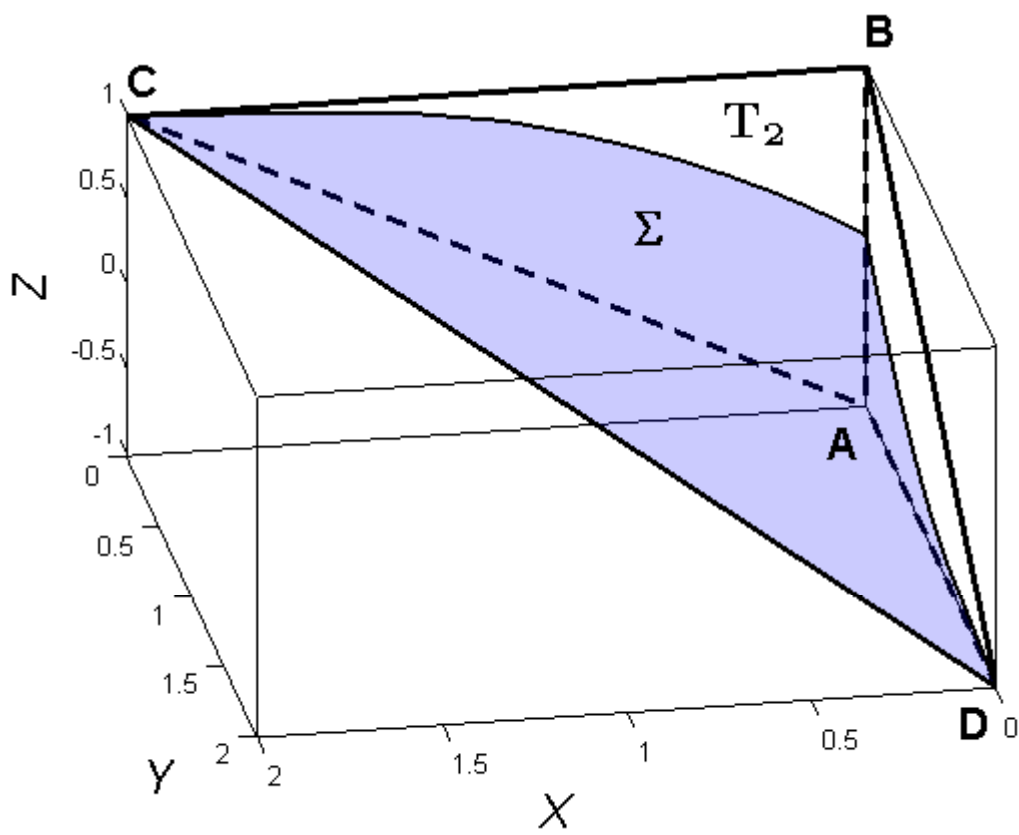


Fig. 3

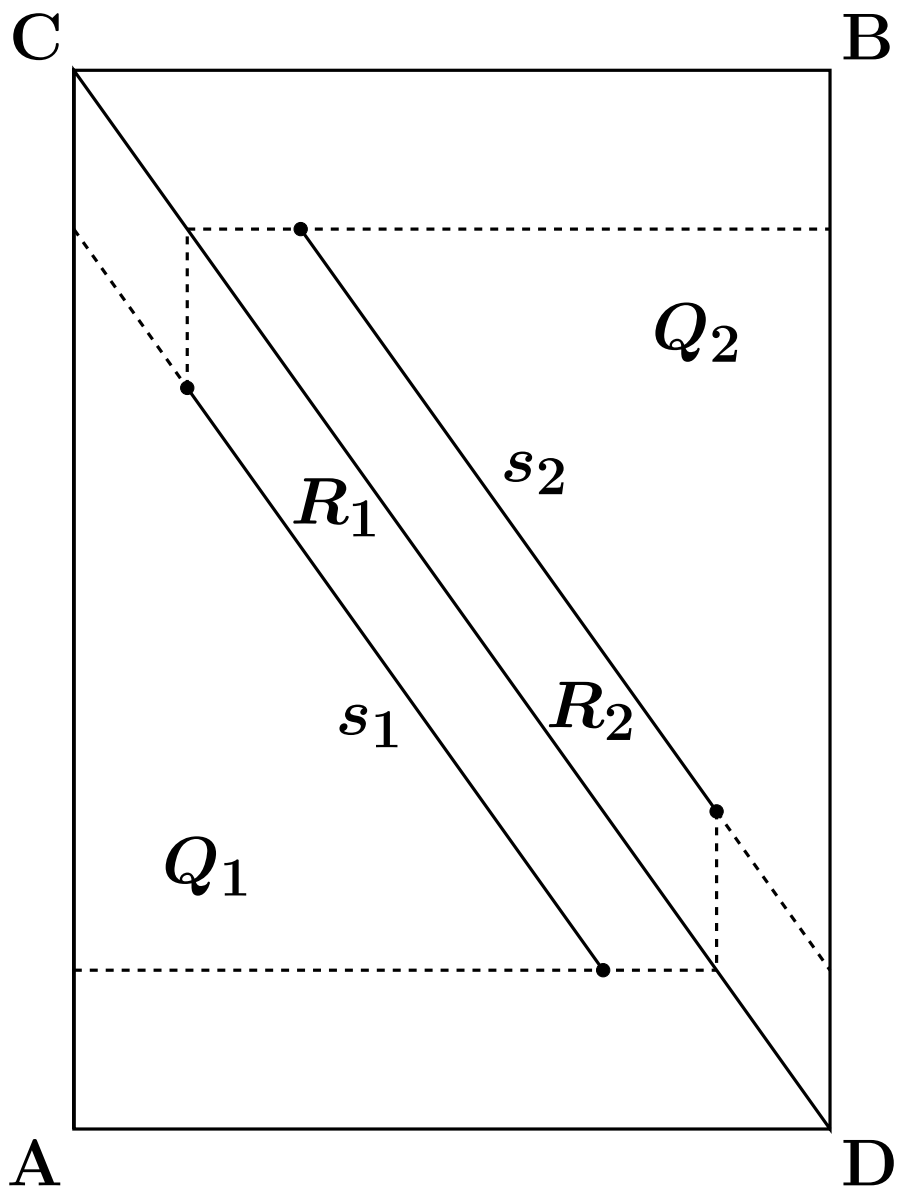


Fig. 4

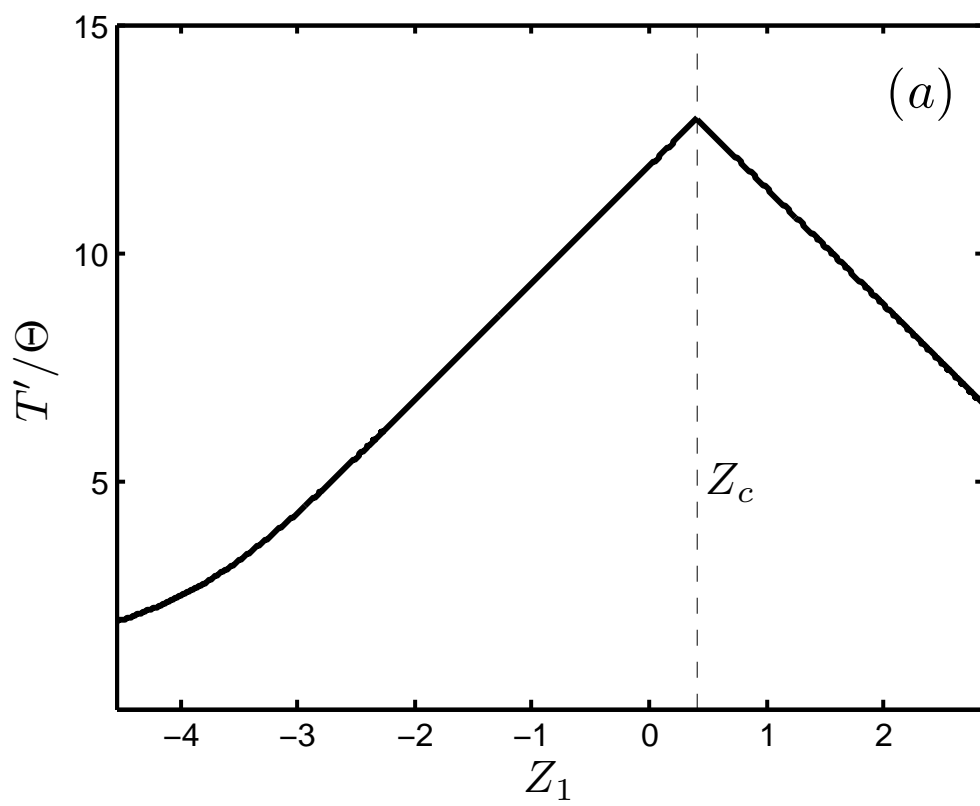


Fig. 5a

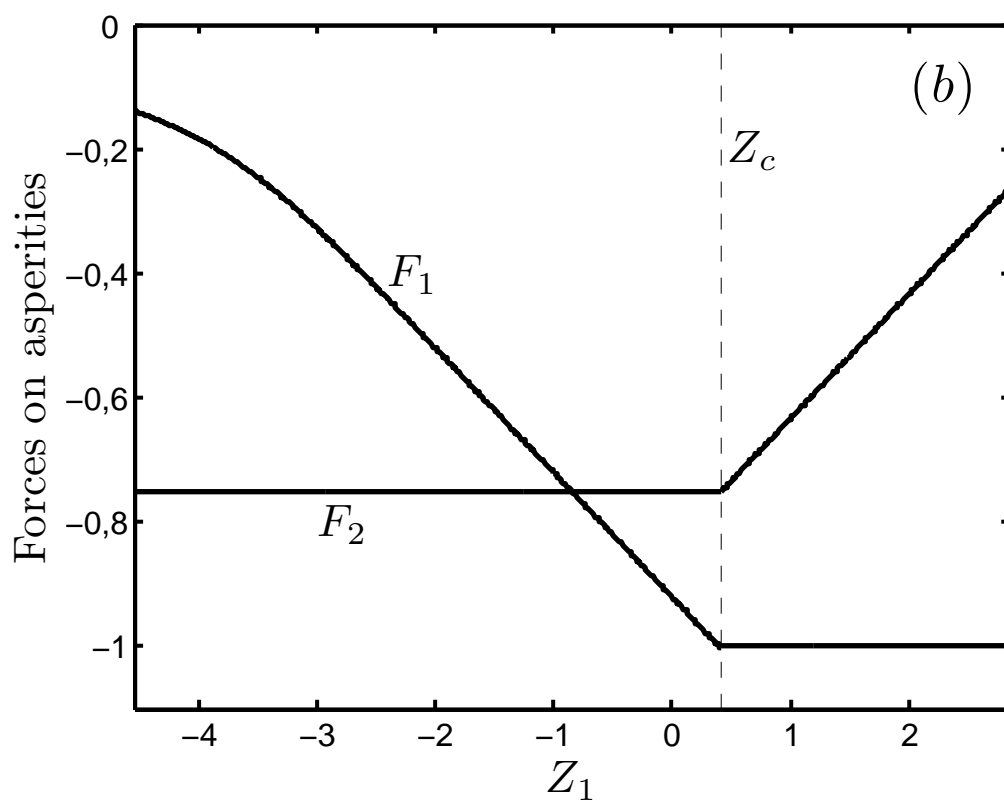


Fig. 5b

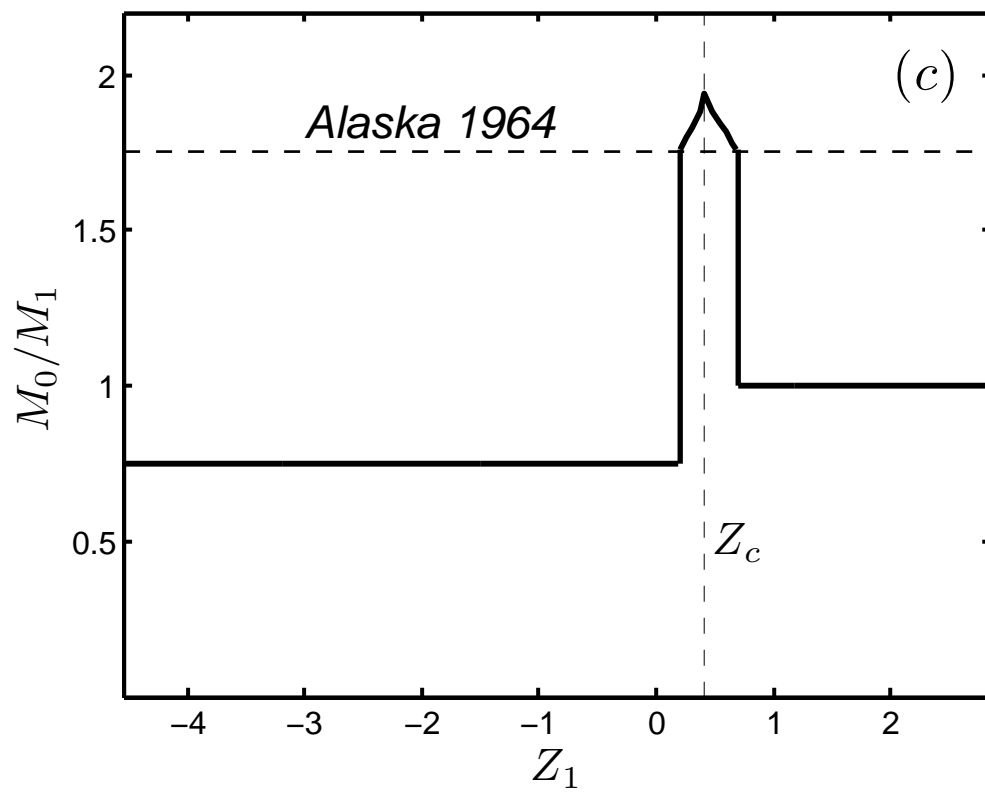


Fig. 5c

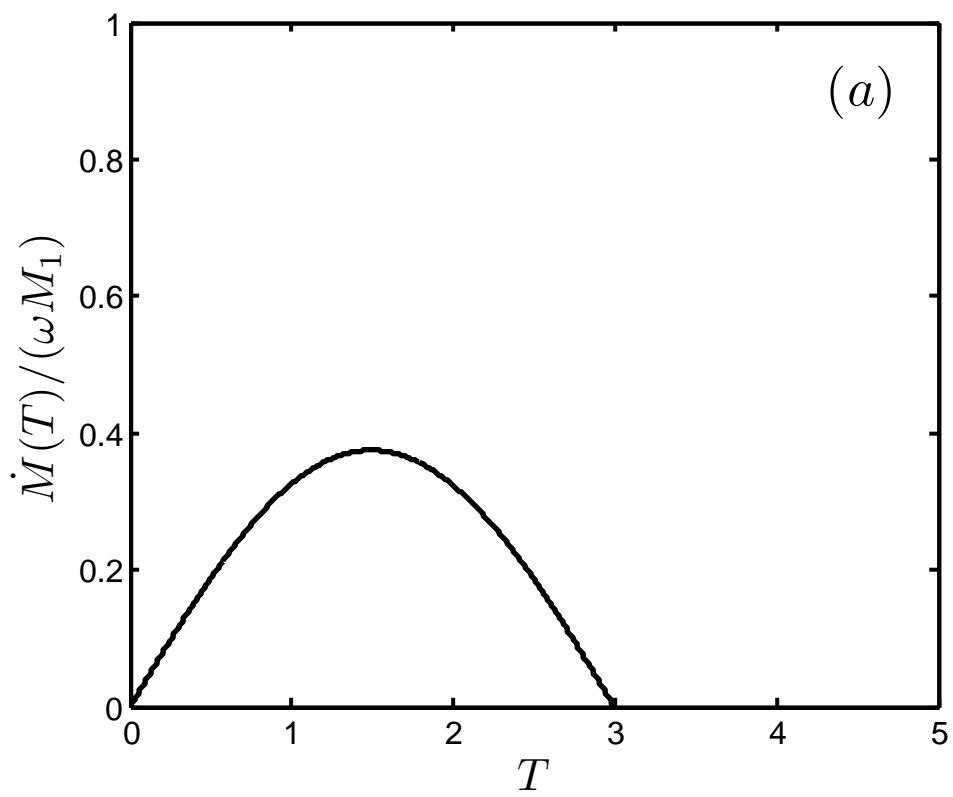


Fig. 6a

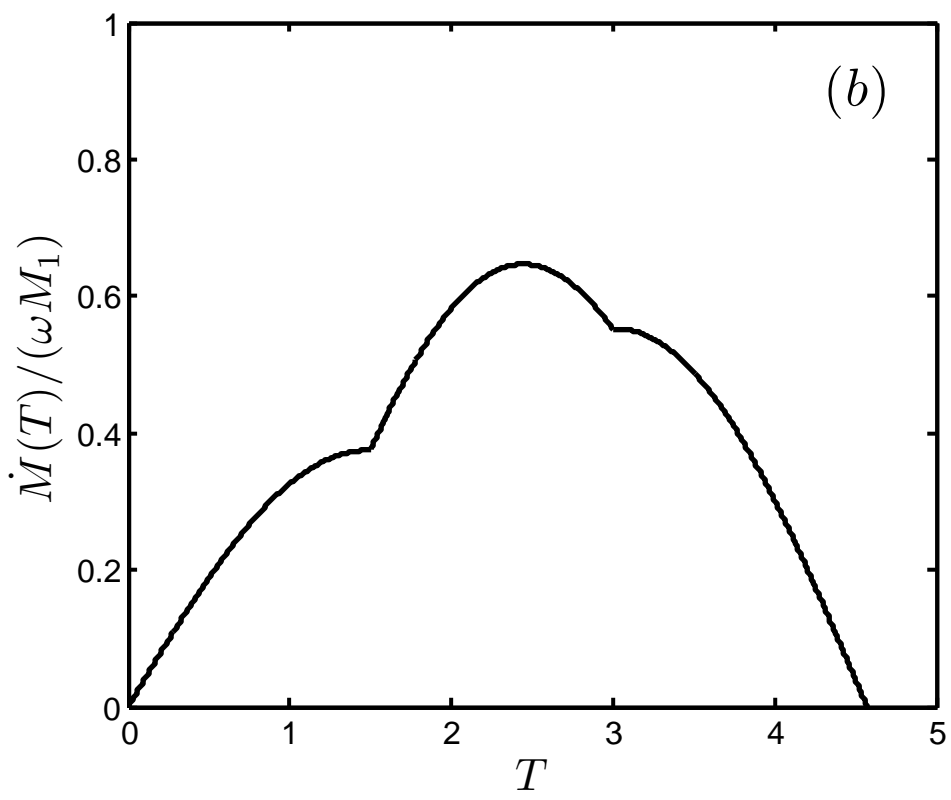


Fig. 6b

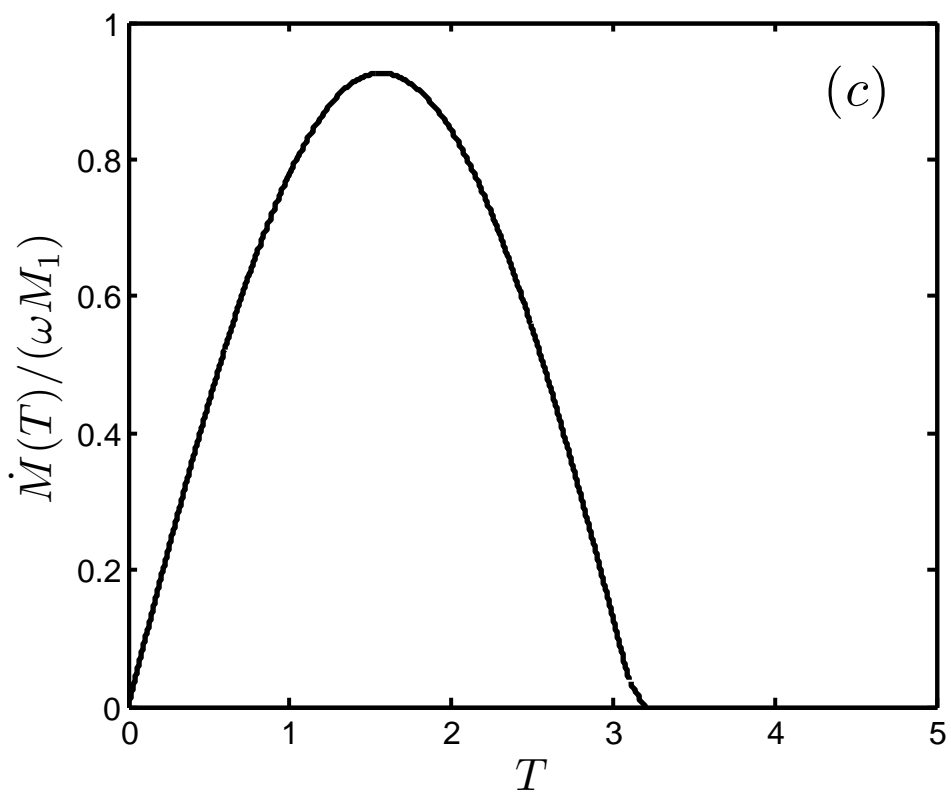


Fig. 6c

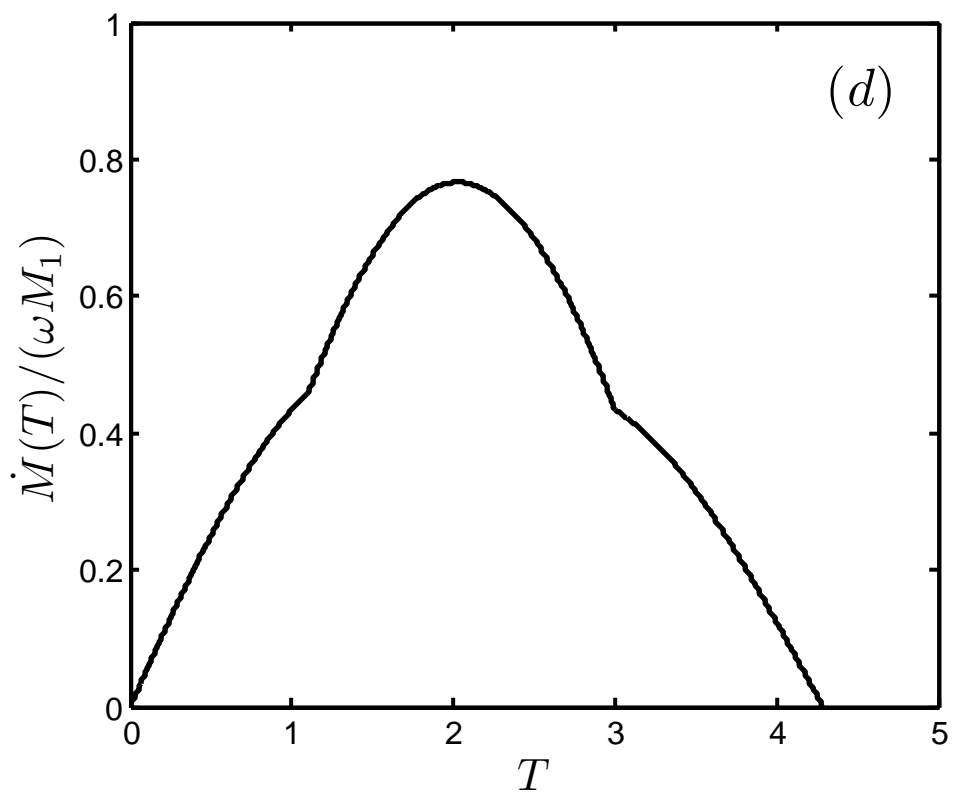


Fig. 6d

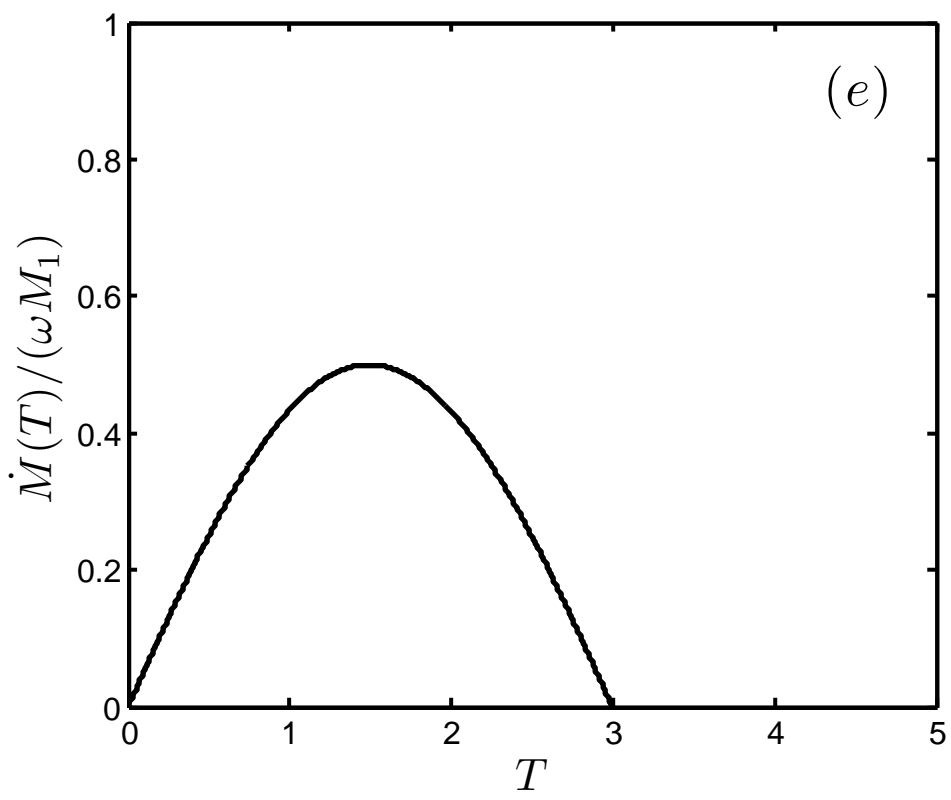


Fig. 6e